Impact of Airborne Doppler Radar Data Assimilation on the Numerical Simulation of Intensity Changes of Hurricane Dennis near a Landfall

ZHAOXIA PU AND XUANLI LI

Department of Atmospheric Sciences, University of Utah, Salt Lake City, Utah

JUANZHEN SUN

National Center for Atmospheric Research, Boulder, Colorado

(Manuscript received 27 February 2009, in final form 15 May 2009)

ABSTRACT

Accurate forecasting of a hurricane's intensity changes near its landfall is of great importance in making an effective hurricane warning. This study uses airborne Doppler radar data collected during the NASA Tropical Cloud Systems and Processes (TCSP) field experiment in July 2005 to examine the impact of airborne radar observations on the short-range numerical simulation of hurricane track and intensity changes. A series of numerical experiments is conducted for Hurricane Dennis (2005) to study its intensity changes near a landfall. Both radar reflectivity and radial velocity–derived wind fields are assimilated into the Weather Research and Forecasting (WRF) model with its three-dimensional variational data assimilation (3DVAR) system. Numerical results indicate that the radar data assimilation has greatly improved the simulated structure and intensity changes of Hurricane Dennis. Specifically, the assimilation of radar reflectivity data shows a notable influence on the thermal and hydrometeor structures of the initial vortex and the precipitation structure in the subsequent forecasts, although its impact on the intensity and track forecasts is relatively small. In contrast, assimilation of radar wind data results in moderate improvement in the storm-track forecast and significant improvement in the intensity and precipitation forecasts of Hurricane Dennis. The hurricane landfall, intensification, and weakening during the simulation period are well captured by assimilating both radar reflectivity and wind data.

1. Introduction

Hurricanes are one of the nature's most intense phenomena and one of the coastal resident's greatest fears. They threaten the maritime industry, devastate coastal regions, and cause floods and erosion inland through torrential rainfall, high winds, and severe storm surges. As suggested by Landsea (1993), hurricane damage increases exponentially with the low-level wind speed. Therefore, accurate forecasting of hurricane intensity changes near their landfall is of great importance for effectively warning the public and reducing economic damage and deaths.

Over the last two decades, the hurricane-track forecast has been improved significantly. However, the intensity forecast remains a great challenge in operational and research communities. According to Rogers et al. (2006), the official 48-h hurricane-track forecast error has reduced by 45% in the past 15 years, whereas the intensity forecast error has decreased by only 17%. They suggest that the major reasons for the lag in the skill of the hurricane intensity forecast include 1) inaccurate storm initial structure in numerical models, 2) limitations in the numerical modeling systems (e.g., physics parameterizations), and 3) inadequate understanding of the physics and the development of hurricanes.

To better understand hurricane structure and intensity change, field experiments, such as the annual National Oceanic and Atmospheric Administration (NOAA) Hurricane Field Program (Aberson and Etherton 2006), the National Aeronautics and Space Administration (NASA) Convective and Moisture Experiment (Kakar et al. 2006), and the 2005 Hurricane Rainband and Intensity Change Experiment (Houze et al. 2006), have been conducted to collect data during intensive observing

Corresponding author address: Dr. Zhaoxia Pu, Department of Atmospheric Sciences, University of Utah, 135 S 1460E, Rm. 819, Salt Lake City, UT 84112.
E-mail: zhaoxia.pu@utah.edu

DOI: 10.1175/2009JAS3121.1

periods. During July 2005, NASA, in collaboration with NOAA, executed the Tropical Cloud Systems and Processes (TCSP) field experiment (Halverson et al. 2007) based in Costa Rica. The goal of this experiment was to improve the understanding of tropical cyclogenesis and intensity change. During TCSP, many remotely sensed datasets were collected, including regular satellite and aircraft observations. With multiple types of observational data, TCSP offered an opportunity to study not only tropical cyclone development in detail but also the impact of remotely sensed and in situ data on mesoscale forecasts of tropical cyclones. A previous study by Pu et al. (2008) proved that aircraft dropsonde and satellite wind data have improved the large-scale and mesoscale environmental conditions of tropical cyclones and thus have resulted in a positive impact on tropical cyclone track and intensity forecasts. In this study, we further examine the impact of airborne Doppler radar data on hurricane intensity forecasts.

It has been recognized that the accurate forecasts of hurricane structure and intensity changes are closely related to the storm inner-core thermal and dynamic structures and their evolution (Jordan 1961; Franklin et al. 1988; Kossin and Eastin 2001; Houze et al. 2006; Rogers et al. 2006; Houze et al. 2007). However, most available satellite data over the hurricane inner-core region are contaminated by heavy precipitation. This produces uncertainties in representing the hurricane structures. Because of a lack of reliable observations near the hurricane inner core, hurricane storm-scale structures are usually not well represented in the numerical simulations (e.g., Wang 2002; Persing and Montgomery 2003; Hendricks et al. 2004; Montgomery et al. 2006; Pu et al. 2009). Thus, forecasting hurricane intensity change, especially the weakening of a hurricane near its landfall, becomes a challenging problem in research and operational practice.

Recent operations of Doppler radar have brought opportunities to sample the thermodynamics, microphysics, and dynamic characteristics of mesoscale systems. With data at high spatial and temporal resolution, airborne Doppler radar can reveal detailed structural features of mesoscale storms. Studies indicated that the assimilation of Doppler radar data can improve the short-term prediction of dynamic, hydrometeor, and precipitation structures for convective systems (Weygandt et al. 2002; Sun 2005). For instance, Sun and Crook (1998) showed that assimilating radar reflectivity and radial wind has improved the precipitation and storm evolution prediction for a supercell storm because of more realistic initial thermal and microphysics features. Xiao et al. (2005) demonstrated a positive impact of radar velocity data on the short-term prediction of a heavy rainfall.

Recent studies have demonstrated that these radar data are useful in studying hurricanes. Xiao et al. (2007) developed a radar reflectivity data assimilation scheme within a three-dimensional variational data assimilation (3DVAR) system of the fifth-generation Pennsylvania State University–NCAR Mesoscale Model (MM5), version 5. The observational data from the onshore Doppler radar at Jindo, South Korea, were assimilated for the prediction of the landfalling Typhoon Rusa (2002). A noticeable improvement in the short-range prediction of the precipitation was produced by the radar data assimilation. Zhao and Jin (2008) assimilated observations from five Weather Surveillance Radar-1988 Doppler (WSR-88D) radars for Hurricane Isabel (2003). With the Navy's Coupled Ocean–Atmosphere Mesoscale Prediction System (COAMPS), they assimilated radar reflectivity and radial velocity data every 1 h within a 4-h assimilation window. The assimilation of the radar data produced an improved structure of Hurricane Isabel. Specifically, radar data assimilation corrected the overestimates of hydrometeors from the numerical simulation. The inner core and outer rainbands of the hurricane were also better organized. The forecast of accumulated precipitation during and after hurricane landfall were also improved.

In both aforementioned hurricane studies, only ground-based radar data were used. Because hurricanes usually generate and develop over the ocean, there has been increasing interest in the use of airborne Doppler radar to study hurricane structures (Marks 2003). With very high resolution, about 1–2 km in the horizontal and 0.5 km in the vertical directions, airborne Doppler radars mostly represent the inner wind, moisture, and hydrometeor structure within the hurricane eyewall. During the TCSP, NOAA P-3 aircraft flew over several tropical cyclones. With Doppler radar on board, radar reflectivity and radial velocity observations were collected to sample hurricane inner structures. Considering the potential increase of these airborne Doppler radar data in future hurricane research and operations, it is our purpose to examine the impact of airborne Doppler radar data assimilation on predicting hurricane intensity changes near the landfall events. Based on the data availability, Hurricane Dennis (2005) during the TCSP field program was chosen for a case study. The usefulness of airborne Doppler radar reflectivity and radial velocity in better representing the hurricane inner-core structure and improving hurricane intensity forecasts near its landfall will be investigated.

The paper is organized as follows: a brief overview on Hurricane Dennis and the airborne Doppler radar data is described in section 2. Methods of radar data assimilation and experimental design are described in

section 3. The numerical results are discussed in section 4. Summary and concluding remarks are made in section 5.

2. Description of Hurricane Dennis and Doppler radar data

a. A brief overview of Hurricane Dennis (2005)

According to Beven (2005), Hurricane Dennis developed from a tropical wave near the coast of Africa on 29 June 2005. It became a tropical storm on 5 July, reached hurricane strength early on 7 July, and then rapidly intensified into category 4 strength before making landfall near Puntadel Ingles in southeastern Cuba around 0300 UTC 8 July. Dennis weakened to a category 3 hurricane while passing across southeastern Cuba. Once offshore in the Gulf of Guacanayabo, the hurricane moved west-northwestward, parallel to the south coast of Cuba, and it again intensified to category 4 status. Maximum sustained winds reached a peak of 67 m s^{-1} at 1200 UTC 8 July and then decreased to 62 m s^{-1} before Dennis made landfall near Punta Mangles Altos, Cuba, around 1845 UTC that day. Dennis then traversed a long section of western Cuba and weakened significantly. The maximum sustained winds decreased to 38 m s^{-1} by the time the center left the island. Once offshore, the hurricane intensified again into a category 4 hurricane. On 9 July, Dennis moved into the Gulf of Mexico. Late on 10 July, Dennis made landfall on Santa Rosa Island, Florida.

Based on the data availability and the purpose of this paper, this study focuses on the time period between 0600 UTC 8 July and 0000 UTC 9 July 2005, when Dennis experienced intensity changes following a pattern of intensification, slow weakening, and deep weakening before and during its landfall near Punta Mangles Altos, Cuba.

b. Airborne Doppler radar data

During the NASA TCSP field experiment, the NOAA P-3 aircraft flew into Hurricane Dennis to observe its development. Airborne Doppler radar reflectivity and velocity data were collected by a lower-fuselage radar and a tail radar aboard the NOAA P-3 aircraft.

The reflectivity and velocity data used in this study are the combined radar sweeps within an area of 180 km around the storm center at a horizontal resolution of 2 km. The NOAA/Hurricane Research Division (HRD) has conducted an automatic quality control for these data and derived the horizontal wind components u and v from radial velocity data. More detailed descriptions of the retrieved algorithm and quality-control techniques can be found in Gamache 2005 and Gao et al. 1999. Figure 1 illustrates the samples of airborne Doppler radar reflectivity and the u and v wind components for Hurricane Dennis at the level of 4 km at 0600 UTC 8 July 2005.

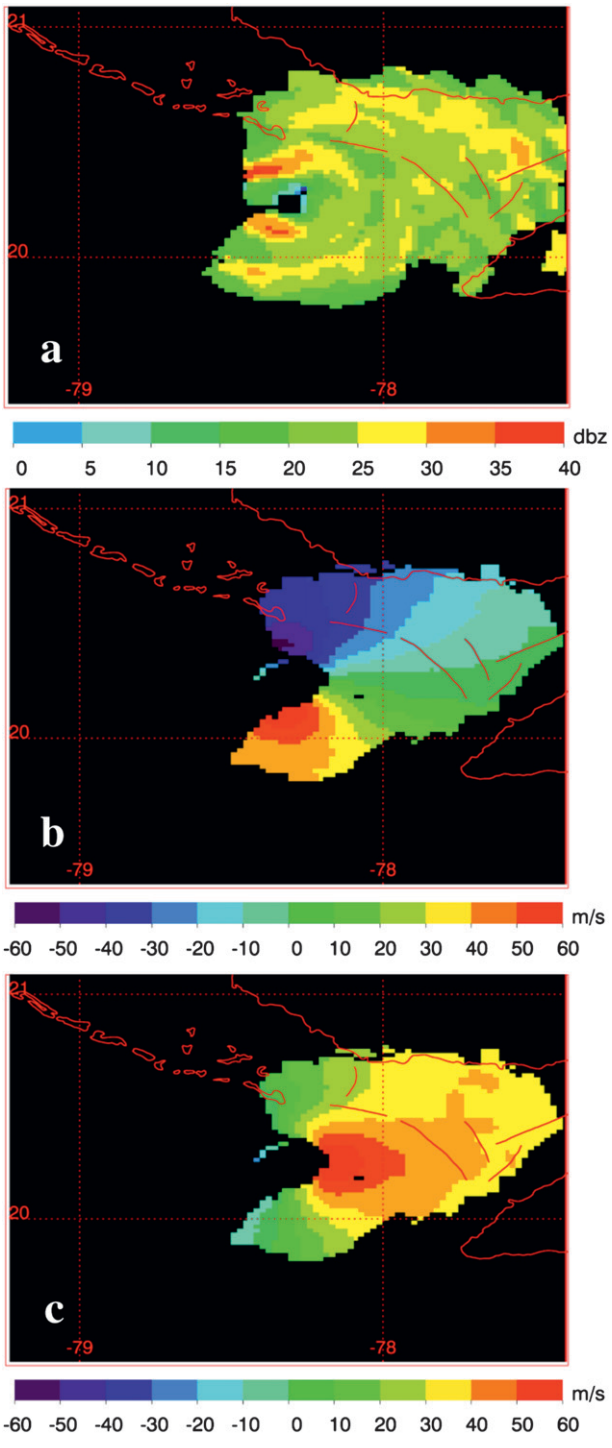

FIG. 1. A sample of composites (a) reflectivity, (b) u component wind, and (c) v component wind at 4-km level from the airborne Doppler radar at 0600 UTC 8 Jul 2005.

Figure 2 shows the number of the radar observations at the different vertical levels at the same time. It is apparent that most of the radar data are distributed between the altitudes of 1 and 10 km.

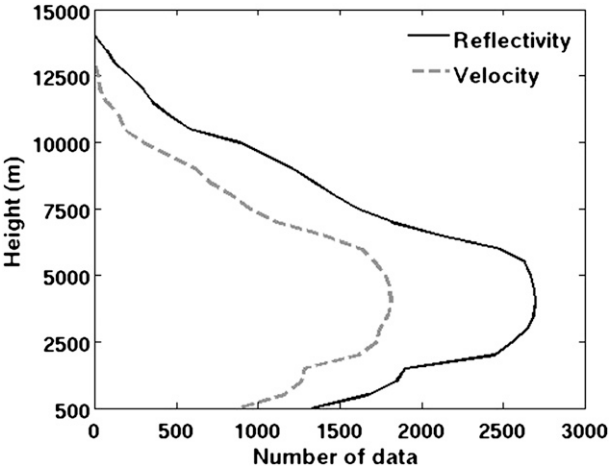

FIG. 2. The vertical distribution of the number of the radar observational data around 0600 UTC 8 Jul 2005.

3. Assimilation method and experimental design

a. WRF model and its 3DVAR system

The Weather Research and Forecasting (WRF) model is a new generation mesoscale numerical weather prediction system. It is designed to serve both operational forecasting and atmospheric research needs. The WRF model features multiple dynamic cores. This study employs the Advanced Research WRF model (ARW-WRF).

The ARW-WRF is based on an Eulerian solver for the fully compressible nonhydrostatic equations, cast in flux conservation form and using a mass (hydrostatic pressure) vertical coordinate. The solver uses a third-order Runge–Kutta time integration scheme coupled with a split-explicit second-order time integration scheme for the acoustic and gravity wave modes. Fifth-order upwind-biased advection operations are used in the fully conservative flux divergence integration; second–sixth-order schemes are run-time selectable. The ARW-WRF carries multiple physical options for cumulus, microphysics, planetary boundary layer (PBL), and radiation physical processes. Details of the model are provided in Skamarock et al. (2005).

Along with the ARW-WRF, a 3DVAR system was developed based on the MM5 3DVAR system (Barker et al. 2004a,b). The 3DVAR system provides an analysis $\mathbf{x}^a$ via the minimization of a prescribed cost function $J(\mathbf{x})$:

$$J(\mathbf{x}) = J^b + J^o = \frac{1}{2}(\mathbf{x} - \mathbf{x}^b)^{\mathrm{T}}\mathbf{B}^{-1}(\mathbf{x} - \mathbf{x}^b) + \frac{1}{2}\sum_{i=0}^{n}(\mathbf{y} - \mathbf{y}_i^0)^{\mathrm{T}}\mathbf{O}_i^{-1}(\mathbf{y} - \mathbf{y}_i^0), \quad (3.1)$$

where the analysis $\mathbf{x} = \mathbf{x}^a$ represents an a posteriori maximum likelihood (minimum variance) estimate of the true state of the atmosphere given two sources of data: the background (previous forecast) $\mathbf{x}^b$ and observations $\mathbf{y}^o$ (Lorenc 1986). The analysis fit to these data is weighted by estimates of their errors: $\mathbf{B}$ and $\mathbf{O}$ are the background and observational error covariance matrices, respectively. Here, $\mathbf{y} = H(\mathbf{x})$ and H is a linear or nonlinear operator used to transform the gridpoint analysis $\mathbf{x}$ to observational space and type. In Eq. (3.1), i denotes each type of observational data and n represents the total number of data types.

The configuration of the WRF 3DVAR system is based on a multivariate incremental formulation (Courtier et al. 1994). The preconditioned control variables were streamfunction, velocity potential, unbalanced pressure, and total water mixing ratio. Statistics of the differences between 24- and 12-h forecasts were used to estimate background error covariance with the so-called National Meteorological Center [NMC; now known as the National Centers for Environmental Prediction (NCEP)] method (Parrish and Derber 1992; Wu et al. 2002; Barker et al. 2004a). Horizontally isotropic and homogeneous recursive filters were applied to horizontal components of background error. The vertical component of background error was projected onto a climatologically averaged (in time, longitude, and latitude) eigenvector of vertical error estimated with the NMC method. A detailed description of WRF 3DVAR can be found in Barker et al. (2004a,b).

Because the Doppler radar radial velocity used in this study has already been derived into component winds (u and v), which are the same as the analysis variables, assimilation of the wind data can directly apply Eq. (3.1). However, assimilation of radar reflectivity requires additional forward operator to associate the model hydrometeors with the radar reflectivity.

b. Radar reflectivity assimilation

Radar reflectivity measures the radar's signal reflected by precipitation hydrometeors. To assimilate radar reflectivity data, the WRF 3DVAR system should be able to produce the increments of the hydrometeors (e.g., rainwater mixing ratio). However, the NMC method is not appropriate to perform the background error statistics for the rainwater mixing ratio, because it will result in zero errors in most of the grid points in the model domain. Therefore, following Xiao et al. (2007), we chose total water mixing ratio as a control variable and conducted the background error statistics.

Because the total water mixing ratio is used as a control variable, partitioning of the moisture and hydrometeor increments is necessary in the 3DVAR system.

To build the relationship among rainwater, cloud water, moisture, and temperature, a warm rain physical process (following Dudhia 1989) is adopted for the radar reflectivity data assimilation. This warm rain process includes the condensation of water vapor into cloud water, accretion of cloud water by rain, automatic conversion of cloud water to rain, and evaporation of rain to water vapor (for details, see Kessler 1969; Xiao et al. 2007). Then, according to Sun and Crook (1997), when assuming the Marshal–Palmer distribution of drop size for rainwater and $n_0 = 8 \times 10^6$ mm^{-4}, the radar reflectivity (in dBZ) can be estimated from rainwater mixing ratio q_r by

$$Z = 43.1 + 17.5 \log(\rho q_r), \tag{3.2}$$

where ρ is air density. From Eq. (3.2), the model simulated radar reflectivity will be obtained. This enables us to get the innovation vectors [observations minus first guess; namely, the second term of Eq. (3.1)] in the 3DVAR system. Thus, the radar reflectivity data can be assimilated into the ARW-WRF model. The tangent linear and its adjoint of the scheme were developed and incorporated into WRF 3DVAR system (Xiao et al. 2007). Although the control variable is the total water mixing ratio, the water vapor mixing ratio, cloud water, and rainwater mixing ratio increments are produced through the partitioning procedure during the 3DVAR minimization.

c. Experimental design

Numerical simulations are conducted using two-way interactive nested domains with the ARW-WRF model. Figure 3 shows the location of the model domains. The outer domains, A and B, have the horizontal resolutions of 36 and 12 km and start at 1800 UTC 4 July 2005. The inner domains, C (4-km grid spacing) and D (1.33-km grid spacing), start at 0500 UTC 7 July 2005. The innermost domain D is a movable domain for keeping the storm near the center of the domain (from D1 to D2, as shown in Fig. 3). The model physics options include the Rapid Radiative Transfer Model (RRTM; Mlawer et al. 1997) of longwave radiation, Dudhia shortwave radiation (Dudhia 1989), the WRF single-moment, six-class scheme (WSM6) microphysics (Hong and Lim 2006), Grell–Dévényi ensemble cumulus (Grell and Dévényi 2002), and Mellor–Yamada–Janjic (MYJ) PBL scheme (Janjic 2002). The cumulus scheme is only used for the outer domains A and B. The model vertical structure is comprised of 31 σ levels with the top of the model set at 50 hPa, where $\sigma = (p_h - p_{\rm ht})/(p_{\rm hs} - p_{\rm ht})$. Although p_h is the hydrostatic component of the pressure, $p_{\rm hs}$ and $p_{\rm ht}$ refer to values of the pressure along the surface and top boundaries, respectively. The σ levels are placed close together in the low levels (below 500 hPa) and are relatively coarsely spaced above.

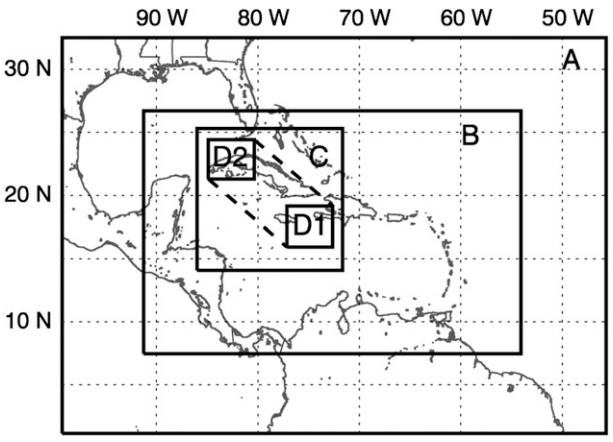

FIG. 3. Model domains for Hurricane Dennis. Domain A is the 36-km grid. The inner domains B, C, and D are the nested 12-, 4-, and 1.33-km grids. Domain D moved 4 times (from D1 to D2) during the numerical simulation to keep the storm near the center of the domain.

The control experiment starts from 0000 UTC 4 July 2005 in order to spin up the vortex. The data from the NCEP global final analysis (FNL) on a 1° × 1° grid are used to provide initial and boundary conditions. To make a more realistic control forecast, the sounding data from the Atmospheric Infrared Sounder (AIRS) on the NASA *Aqua* satellite are assimilated at 1800 UTC 6 July and 0600 UTC 7 July 2005, and the Quick Scatterometer (QuikSCAT) ocean surface vector winds are assimilated at 0000 UTC 7 July 2005. Then, the forecast for the control experiment continues until 0000 UTC 9 July 2005, whereas data assimilation experiments take the forecast at 0500 UTC 8 July as the first guess field to begin the radar data assimilation cycle. Three experiments are performed using the WRF 3DVAR system to investigate the impact of the Doppler radar data on the simulation of Hurricane Dennis. Among these three experiments, the first experiment (RD1) only assimilates radar reflectivity data; the second experiment (RD2) only assimilates the radar radial velocity–derived wind components; and both reflectivity and wind data are assimilated in the third experiment (RD3). In all three experiments, data assimilation is cycled every 30 min within a 1-h assimilation window from 0500 to 0600 UTC 8 July 2005 for the domains B, C, and D. After the data assimilation, an 18-h forecast is conducted in each experiment from 0600 UTC 8 July to 0000 UTC 9 July 2005. Table 1 lists the data assimilated in each of these different experiments.

TABLE 1. Numerical experiments and the radar data assimilated in the experiments.

Expt	Radar data	Time of data assimilation
CTRL	—	—
RD1	Radar reflectivity	0500, 0530, and 0600 UTC 8 Jul 2005
RD2	Radar wind	0500, 0530, and 0600 UTC 8 Jul 2005
RD3	Radar reflectivity and wind	0500, 0530, and 0600 UTC 8 Jul 2005

Because the radar reflectivity and the radial velocity–derived wind components have been preprocessed and quality controlled by the NOAA/HRD, no additional quality control is conducted before the data assimilation. Inside of 3DVAR, the quality of the wind components (u and v) is further checked by a default quality-control process. The observational errors are prescribed to be 2 m s^{-1} for the radar retrieved u and v wind components and 5 dBZ for the observed radar reflectivity based on statistics of the large sample of the data.

4. Impacts of radar data assimilation on hurricane simulations

To examine the impact of radar data assimilation on numerical simulation of Hurricane Dennis, numerical results from different experiments are compared during the time period between 0600 UTC 8 July and 0000 UTC 9 July 2005.

a. The initial storm structure

Figure 4 shows the sea level pressure (SLP) and surface wind vector fields at the end of the data assimilation experiments (0600 UTC 8 July 2005) compared with the corresponding fields from the control (CTRL) experiment. At the time, Dennis was observed as a category 3 hurricane with minimum SLP (MSLP) of 953 hPa and maximum surface wind (MSW) of 57 m s^{-1}. As shown in Fig. 4, all the experiments overestimate the intensity of Hurricane Dennis. Specifically, CTRL (Fig. 4a) produces a hurricane with the minimum central SLP of 940 hPa and MSW of 65 m s^{-1}. With the assimilation of radar reflectivity data, only slight change in storm intensity is found (Fig. 4b). When the radar wind data are assimilated, the simulated MSW of the hurricane change to 60 m s^{-1}, although the minimum central SLP is still 941 hPa (Fig. 4c). When both radar reflectivity and wind data are assimilated (Fig. 4d), the experiment reproduces an intensity that is much closer to the observed intensity, with MSLP of 946 hPa and MSW of 58 m s^{-1}. In addition, with assimilation of the radar wind components, the position of the hurricane has been modified; compared with CTRL and RD1, the positions of the storm centers in RD2 and RD3 are closer to the observed position (Figs. 4c,d).

Assimilation of radar reflectivity data has significant impacts on the thermo- and hydrometeor structures of the initial vortex. Figure 5 illustrates the difference between RD1 and CTRL at the 850-hPa pressure level for temperature, water vapor mixing ratio, cloud water, and rainwater at the end of the data assimilation period (0600 UTC 8 July 2005). It is apparent that assimilation of radar reflectivity data has modified the temperature and hydrometeor fields, especially in the eyewall and rainband regions. Specifically, an area of negative values in temperature difference at 850-hPa pressure level is seen over the eyewall and northwest inner rainband (Fig. 5a). The water vapor mixing ratio decreased by up to 4 g kg^{-1} near the storm eyewall (Fig. 5b). The cloud water is also changed, especially to the northwest of the eyewall (Fig. 5c). Large decreases in the rainwater mixing ratio appear to the southeast of the eyewall, the inner rainband, and the outer rainband (Fig. 5d).

Significant changes in the wind structures near the hurricane core areas have been obvious after assimilation of the radar wind data. Figure 6 compares the horizontal wind speed, vectors, and vertical velocity at the 850-hPa pressure level between CTRL and RD2. Strong winds in the northeast quadrant and weak winds in the southwest quadrant of the vortex are found in both experiments. However, RD2 produces a stronger horizontal wind than CTRL does in the northeast quadrant of the vortex. Specifically, more areas in the northeast quadrant of the vortex experience strong wind (e.g., exceeding 40 m s^{-1}) in RD2 compared with those in CTRL. In the southwest quadrant, the horizontal wind in RD2 is weaker than that in CTRL. Overall, RD2 generates a stronger asymmetric horizontal wind field than CTRL does. The vertical velocity is also influenced by the radar wind data assimilation. The strongest updraft appears in the west and southwest of the eyewall in CTRL, whereas the strongest convection appears to the north and northwest of the eyewall in RD2 (Figs. 6c,d).

To quantitatively demonstrate the impact of radar data assimilation at different pressure levels at the end of the data assimilation, the root-mean-square (RMS) differences between CTRL and experiments (RD1 and RD2) are calculated. This is defined as

$$\mathrm{RMS} = \sqrt{\frac{\sum_{i=1}^{N}(a_i - o_i)^2}{N}}, \qquad (4.1)$$

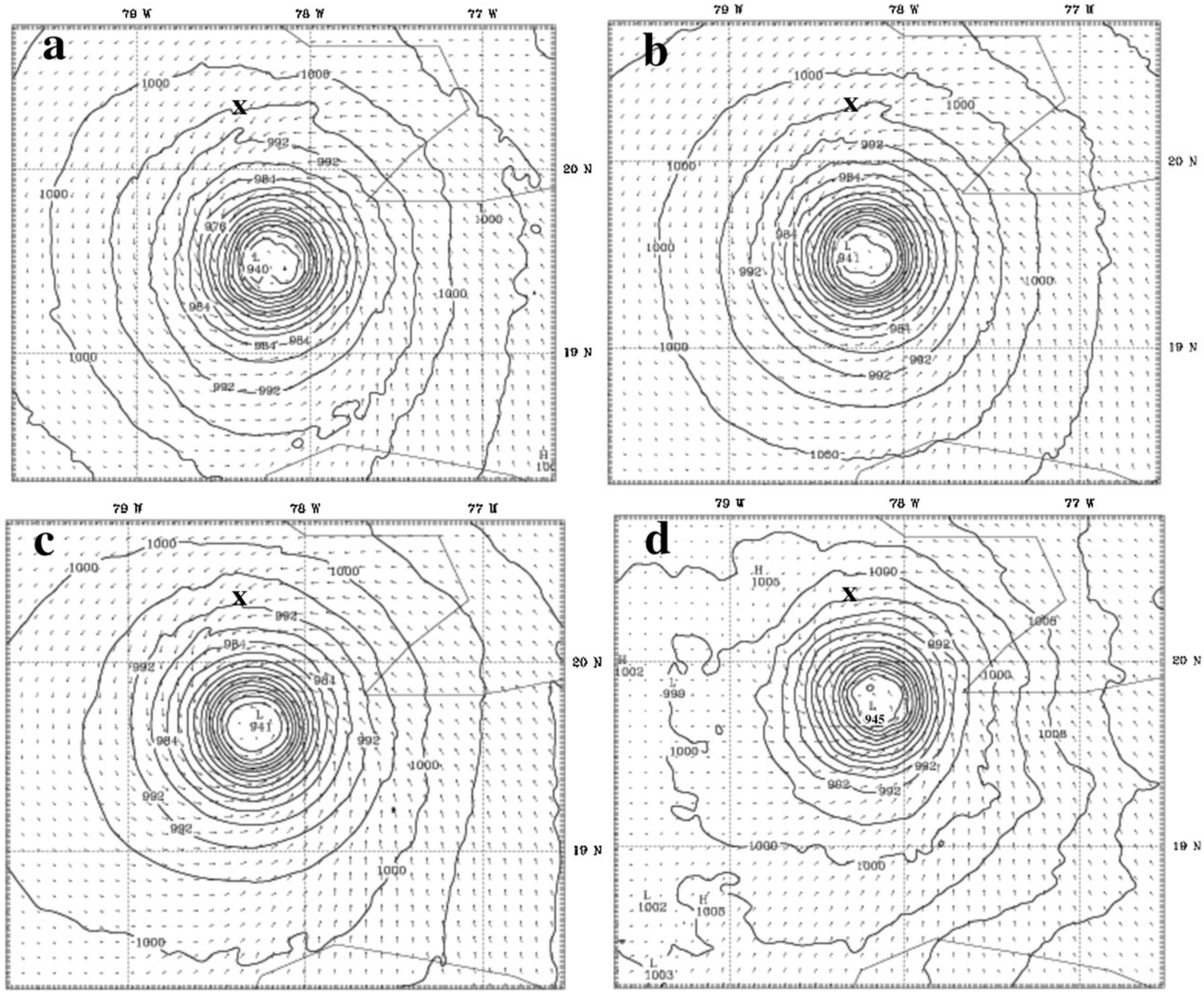

FIG. 4. SLP and surface wind at 0600 UTC 8 Jul 2005 from experiment (a) CTRL, (b) RD1, (c) RD2, and (d) RD3. The 'X' symbols indicate the location of the observed storm center. The maximum wind speeds are (a) 65, (b) 64, (c) 60, and (d) 58 m s^{-1}.

where o_i represents values of temperature T, water vapor mixing ratio q, and wind components u and v from CTRL; a_i represents the values of corresponding analysis variables in experiments RD1 or RD2; and N is the total grid points in domain D. Figure 7 illustrates the root-mean-square differences of T, q, u, and v in domain D (the 1.33-km grid spacing) between CTRL and RD1 and between CTRL and RD2. It is obvious that the assimilation of the radar reflectivity data has a large impact on the thermal and moisture fields but a relatively small impact on the wind fields at all height levels. In contrast, assimilation of wind data has resulted in significant impact on the wind field but relatively small impact on the thermal field and moisture field.

In addition, Fig. 7 shows that the larger modification in wind field from assimilation of radar-derived wind data happens in the low to middle troposphere (600–900-hPa pressure levels) and upper levels of the atmosphere (~250-hPa pressure level). To further examine the impact from assimilation of wind data, Fig. 8 compares the divergence fields from CTRL and RD2 over the hurricane vortex area at both the 250- and 850-hPa pressure levels. It is apparent that assimilation of wind data has resulted in decreases of upper-level divergence and lower-level convergence (negative divergence) in the storm vortex. As a consequence, the overdeepening of the hurricane intensity has been improved by the data assimilation (Fig. 4).

b. Track and intensity forecasts

The data assimilation experiments lead to different forecasts of hurricane track and intensity. Figure 9 compares the forecasted tracks from different experiments

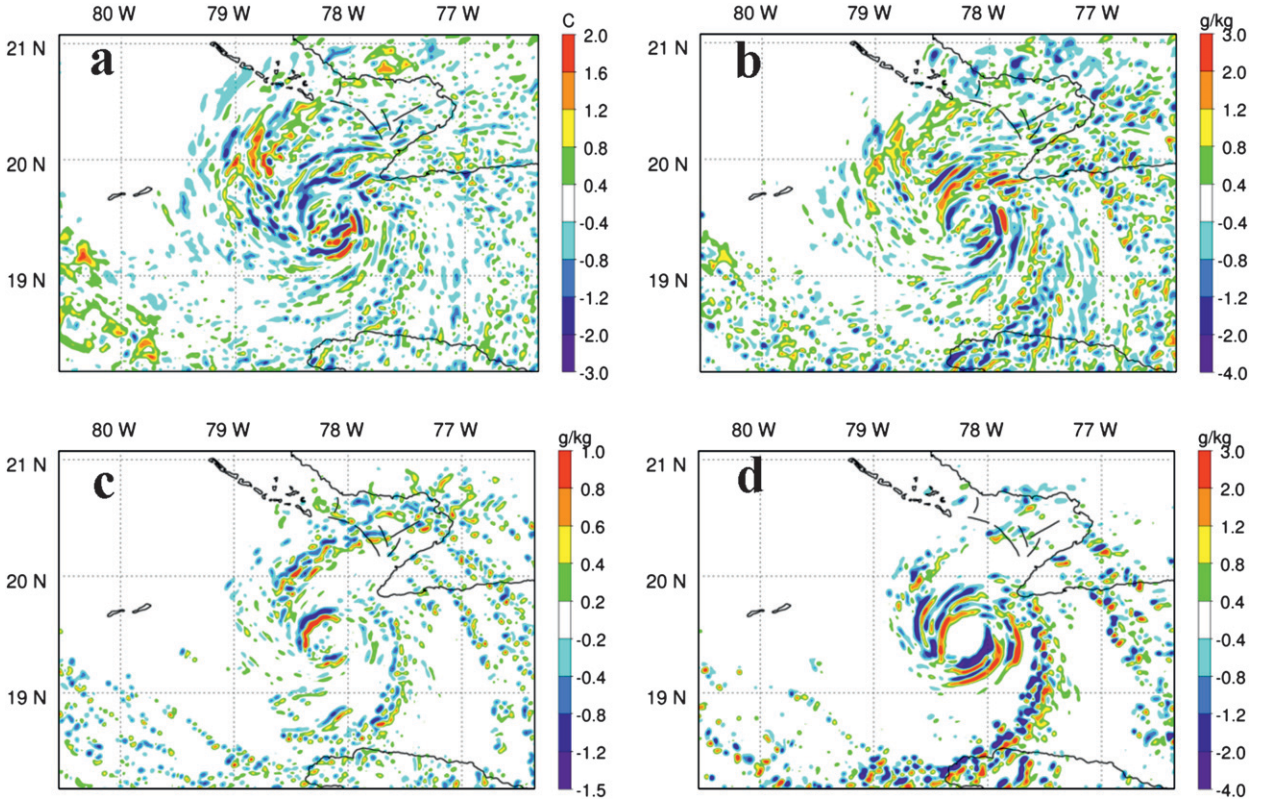

FIG. 5. Differences between the CTRL and RD1 at 850-hPa pressure level for (a) temperature, (b) water vapor mixing ratio, (c) cloud water, and (d) rainwater at 0600 UTC 8 Jul 2005.

with the National Hurricane Center (NHC) best track. The CTRL experiment produces a southeastern bias in the storm track at the beginning and then a southwestern bias in the forecast with large errors, especially in the last 9 h of the forecast. Specifically, the observed storm made landfall near Punta Mangles Altos, Cuba, around 1800 UTC 8 July 2005. However, the CTRL simulation did not capture this landfall event. The radar reflectivity data show only a slight positive impact on the storm track, whereas the simulated track is very similar to CTRL. Assimilation of the radar wind data has resulted in a significant impact on the storm-track forecast. The southern bias in the storm track was greatly improved. Although the forecasted storm missed the landfall near 1800 UTC 8 July, it made a landfall farther west to the observed location at the end of the numerical simulation. When both radar reflectivity and wind data were assimilated, the forecasted hurricane made landfall near 1800 UTC 8 July and almost captured the observed time of landfall, although the landfall location was still farther southwest when compared with the actual landfall location.

Figure 10 illustrates the track errors from different numerical simulations. It shows that the track errors have not decreased much in all experiments, although improvement in track forecasts has been presented in all experiments. This factor may imply that the hurricane-track forecasts do not solely depend on the hurricane initial vortex structures. As the radar data are mostly available near the hurricane vortex, the data assimilation in this study has mainly influenced the vortex structures instead of the large-scale environmental conditions. However, these results still prove that assimilation of radar data does have an impact on the track forecast. In this specific case, radar data assimilation has helped the numerical simulations to shift the storm track northward and thus captured a landfall event.

Figure 11 compares the minimum central SLP and MSW from the NHC best-track data in different experiments. Radar data assimilation shows a notable positive impact on the intensity forecast of Hurricane Dennis. Specifically, the CTRL experiment predicted the deepening of the storm in the first 6 h and the slow weakening in the next 6 h, but it missed the rapid weakening in last 6 h. The forecasted storm intensity is also about 10 hPa deeper than the observed one. A total increase (decrease) of 22 hPa (12 m s^{-1}) in the minimum central SLP (MSW) is observed in the last 12 h,

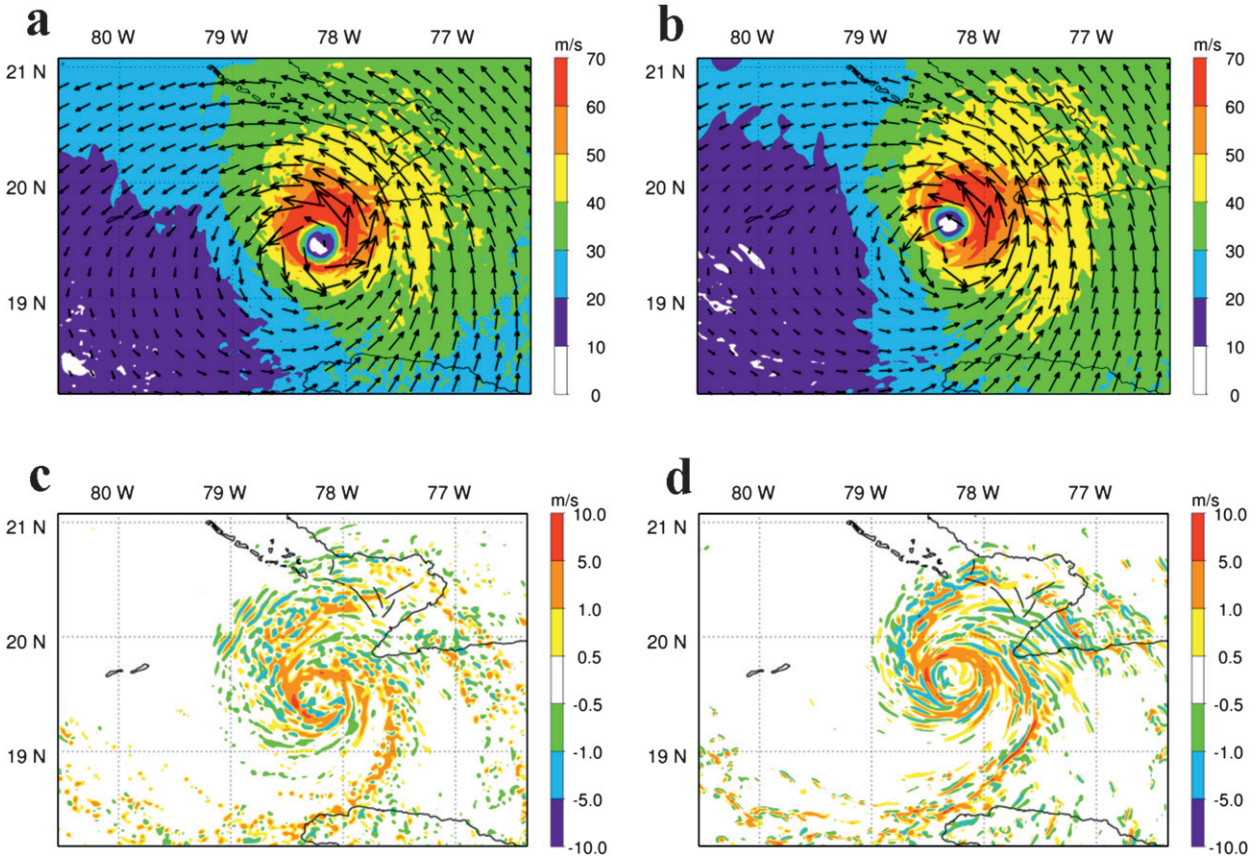

FIG. 6. Horizontal wind speeds and wind vectors for (a) CTRL and (b) RD2 at 850 hPa and vertical velocities at the same level for (c) CTRL and (d) RD2 at 0600 UTC 8 Jul 2005.

and the CTRL only produces an increase (decrease) of 3 hPa (3 m s^{-1}) in the minimum central SLP. Therefore, the weakening rate in CTRL is much slower than that in the observation. When radar data are assimilated into the model, the overdeepening during the whole simulation period is improved. Particularly, assimilation of the radar reflectivity data (experiment RD1) produces a moderate impact on the intensity forecast with the storm

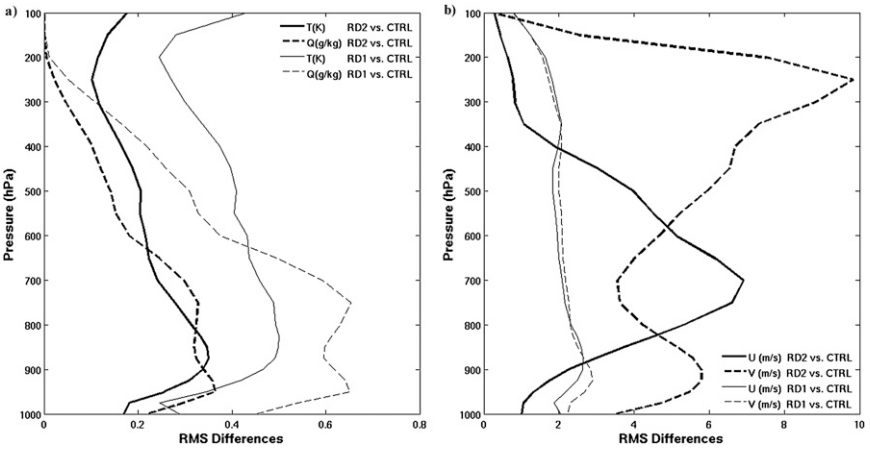

FIG. 7. Vertical distribution of the RMS difference of (a) temperature T and water vapor mixing ratio Q and (b) u and v wind components between CTRL and RD1 and between CTRL and RD2 at 0600 UTC 8 Jul 2005, respectively.

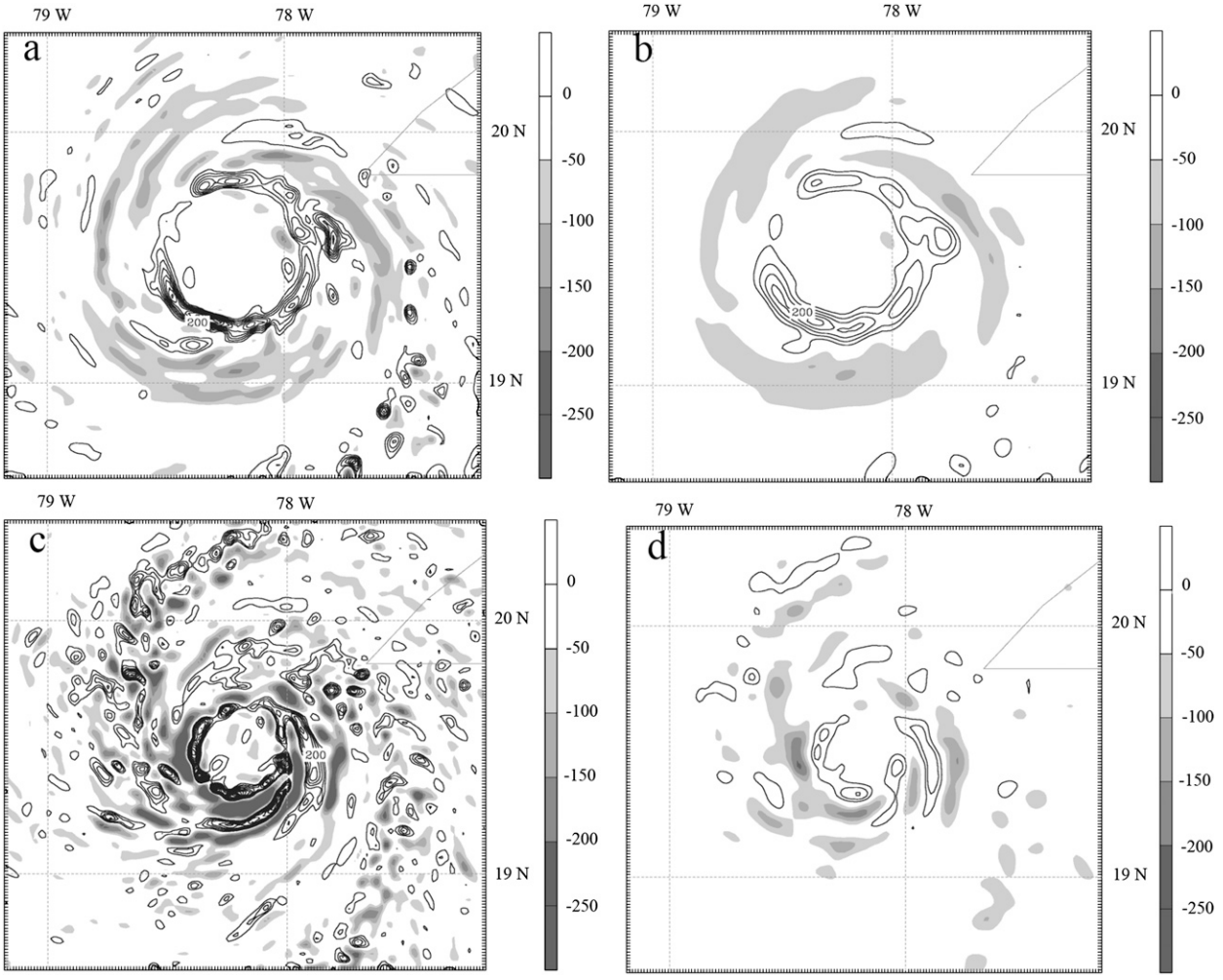

FIG. 8. Divergence fields at (top) 250- and (bottom) 850-hPa pressure levels. (left) CTRL compared with (right) RD2 at 0600 UTC 8 Jul 2005. The line contours denote positive values of the divergence, whereas the shaded contours represent negative values. The contour interval is 50×10^{-5} s^{-1}.

intensity about 4 hPa weaker than that in CTRL at the end of the simulation but closer to the observed intensity. Significant improvement in the overdeepening of the storm intensity forecast is found after the radar wind data are assimilated into the model (experiment RD2). The minimum central SLP at 1200 UTC 8 July 2005 is only 1 hPa different from the observation. Moreover, the weakening of the storm in the last 12 h is also well predicted. At the end of the simulation, the minimum central SLP (MSW) in RD2 is only 5 hPa (3 m s^{-1}) different from the observed one. It is about 22 hPa (10 m s^{-1}) closer to the observed intensity than that in CTRL. When both reflectivity and wind data are assimilated (experiment RD3), the trend and magnitude of storm intensity changes are very similar to those produced by RD2 (Figs. 11a,b).

The majority impact on the intensity forecast from the radar data assimilation can be attributed at least partly to the improved track forecasts. Because the forecasted hurricane in CTRL missed the landfall event and its track was too far from the continent, the hurricane intensity tended to be overly deepened. Assimilation of the radar reflectivity only had a minor impact on the storm-track forecast. Therefore, the improvement in the intensity forecast (weakening process) was also marginal. With assimilation of radar wind information into the model, hurricane-track forecasts have been improved significantly; the landfall event has been well captured. Because of the landfall of the hurricane, the prediction of the weakening of the storm has been greatly improved. In addition, the improved intensity forecast can also be attributed to the improved initial vortex structures. For

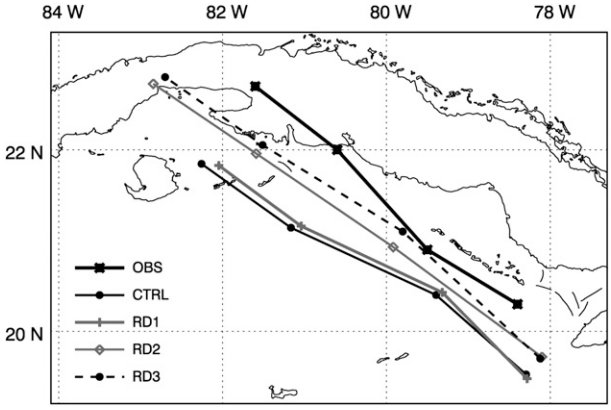

FIG. 9. Storm tracks of Hurricane Dennis (in 6-h intervals) between 0600 UTC 8 Jul and 0000 UTC 9 Jul 2005 from the NHC best-track data and different experiments. The hurricane moves from the southeast to northwest direction during the time period.

instance, as shown in Fig. 8, the intensity and inner-core convergence/divergence conditions in the initial vortex have been improved by the radar data assimilation.

c. *Precipitation*

Heavy rainfall near the hurricane landfall usually causes floods, which is one of the serious natural disasters associated with a hurricane landfall. Accurate forecasts of hurricane precipitation are of great importance. Previous studies (Sun 2005; Xiao et al. 2007) showed that the radar data could have a remarkable impact on the prediction of precipitation. In this section, the impact of the radar reflectivity and wind data on the storm-induced precipitation is examined.

Figure 12 illustrates the hourly rainfall rate from CTRL and the hourly rainfall differences between RD1 and CTRL, RD2 and CTRL, and RD3 and CTRL at 0700 UTC 8 July 2005. They are compared with the NASA Advanced Microwave Scanning Radiometer for Earth Observing System (AMSR-E; on board *Aqua*) satellite sensor observed rain rate at 0702 UTC 8 July 2005. As indicated in Fig. 12b, CTRL captured the major feature of the observed heavy rainfall over the eyewall, inner rainband, and outer rainband. However, it overestimated the rainfall in the eyewall and inner rainband, and it underestimated the rainfall over the outer rainband. With the assimilation of the radar reflectivity data, the amount of rainfall over the eyewall and inner rainband decreased (Fig. 12c). With assimilation of wind data, a great impact on the precipitation structure was found (Fig. 12d). Both the amount and the location of the heavy rainfalls in the eyewall and inner rainband from data assimilation experiments were different from those in CTRL, partly because of the track errors that caused the location differences in the storm centers. When both reflectivity and wind data were assimilated, the eyewall rainfall was produced farther to the north relative to CTRL and closer to the observed features. The amount of rainfall in the inner rainband was decreased in both RD2 and RD3.

The impact of the radar data assimilation on precipitation can be examined quantitatively by comparing the average of the storm-induced rainfall in different experiments. Figure 13 shows the time series of the 3-h accumulated rainfall amount averaged within the area of 250 km from the storm center in different experiments compared with the values from the NASA Tropical Rainfall Measuring Mission (TRMM) 3B42 products (Huffman et al. 2007) between 0600 UTC 8 July and 0000 UTC 9 July 2005. As shown in Fig. 13, all numerical experiments overestimate the storm-induced rainfall. CTRL produces a rainfall amount much larger than that observed by TRMM. The reflectivity data show a positive impact on the rainfall amount forecast in the first 6 h

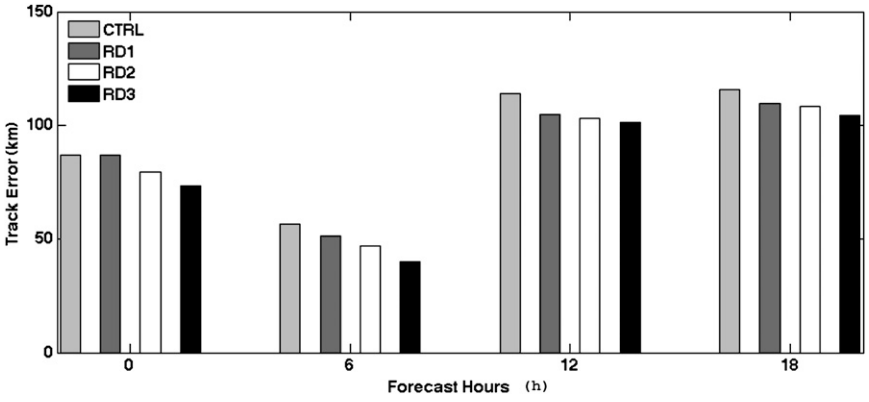

FIG. 10. Forecasted track errors from different experiments between 0600 UTC 8 Jul and 0000 UTC 9 Jul 2005.

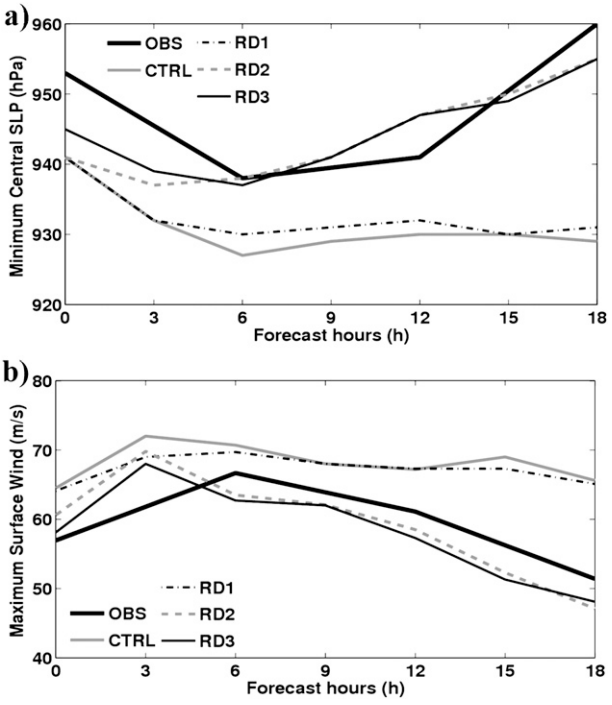

FIG. 11. Time series (6-h intervals) of (a) the minimum central SLP (hPa) and (b) the MSW speed (m s^{-1}) between 0600 UTC 8 Jul and 0000 UTC 9 Jul 2005 from the NHC best-track data (thick line) and different experiments.

of the simulation period. With the radar wind data assimilation (RD2), rainfall amount decreases greatly, especially in the first 12 h of the forecast period. When both reflectivity and wind data are assimilated (RD3), the model produces the rainfall amount that is much closer to the TRMM observation than CTRL and RD1. Larger impact on the precipitation forecasts from the assimilation of wind data may be caused by the improved vortex inner convergence and divergence (Fig. 8) and modified convection conditions (Fig. 6d) in the initial vortex.

5. Summary and concluding remarks

In this study, a series of data assimilation and high-resolution numerical experiments are conducted with the WRF model and its 3DVAR system to simulate Hurricane Dennis (2005). The airborne Doppler radar reflectivity and wind data were assimilated into the model simulation to investigate the intensity change of Dennis near a landfall event during 0600 UTC 8 July–0000 UTC 9 July 2005. The impact of the Doppler radar data on the structure of Dennis was evaluated. The influence of the Doppler radar data on the hurricane forecast was also examined. The results suggest the following:

- The assimilation of radar reflectivity data resulted in a notable influence on the thermal and hydrometeor structures of the hurricane, although only a slight impact was found on the intensity and track forecasts.
- The assimilation of radar wind data has improved the divergence/convergence conditions over the hurricane inner-core area as well as the hurricane inner-convection conditions. Significant influence to the track, intensity, and precipitation forecasts of Hurricane Dennis has been evidenced. Forecasts of hurricane landfall and its intensity changes near the landfall are remarkably improved. In particular, the weakening of the storm during 1200 UTC 8 July–0000 UTC 9 July is well predicted.
- When both the Doppler radar reflectivity and wind data are assimilated, the intensity, track, and precipitation forecasts are further improved, although the results are very similar to the experiment with radar wind data assimilation for this particular case.

Although this study is based only on one case, the impact of airborne Doppler radar reflectivity and wind data on the forecast of hurricane intensity changes has been evidenced. Even with a simple warm rain process, the benefit of reflectivity data assimilation has been proven. Results from this study imply that airborne Doppler radar data are useful in hurricane initialization. While this paper was under revision, we became aware that a series of numerical studies has been conducted by Xiao et al. (2009) with a similar radar data assimilation technique. They have demonstrated that hurricane initialization with airborne Doppler radar data is quite promising toward reducing errors in hurricane intensity forecast.

Meanwhile, the small impact from reflectivity data assimilation in this study may be attributed to the use of a simple warm rain process in the data assimilation. According to previous studies (e.g., Lord et al. 1984; Marks et al. 2007; McFarquhar and Black 2004; McFarquhar et al. 2006; Rogers et al. 2007), ice-phased precipitation could be important on the development of hurricanes. Therefore, a more realistic microphysics scheme needs to be included in the radar data assimilation in the near future. Moreover, the use of the traditional NMC method in mesoscale data assimilation does not specify the background for the hurricane case particularly. Its impact on hurricane-related radar data assimilation should be examined in the future study. In addition, future work will also emphasize the use of more advanced data assimilation techniques (e.g., four-dimensional variational

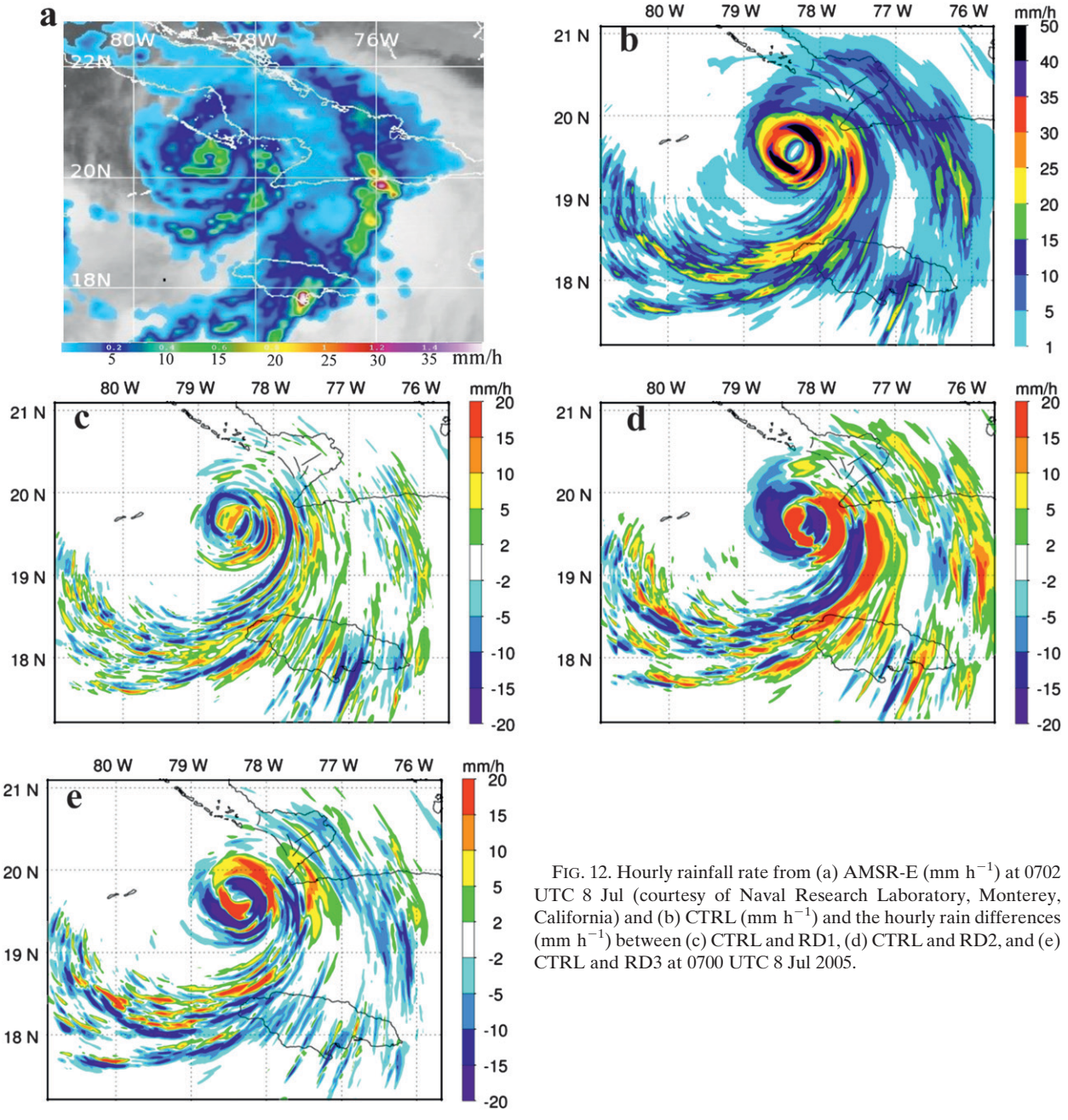

FIG. 12. Hourly rainfall rate from (a) AMSR-E (mm h^{-1}) at 0702 UTC 8 Jul (courtesy of Naval Research Laboratory, Monterey, California) and (b) CTRL (mm h^{-1}) and the hourly rain differences (mm h^{-1}) between (c) CTRL and RD1, (d) CTRL and RD2, and (e) CTRL and RD3 at 0700 UTC 8 Jul 2005.

data assimilation and ensemble Kalman filters) for airborne Doppler radar data assimilation.

Acknowledgments. The authors acknowledge useful discussions with Drs. Ed Zipser, John Horel, and Jay Mace at the University of Utah and Dr. Frank Marks at NOAA/Hurricane Research Division (HRD). The Doppler radar data used in this study were obtained from NOAA/HRD, and the authors are grateful for the helpful comments on the data quality from Drs. Sim Aberson and John Gamache at NOAA/HRD. Review comments from three anonymous reviewers are also greatly appreciated. The authors also would like to express their appreciation to the WRF model working groups for their efforts to develop a mesoscale community model and the 3DVAR data assimilation system. Computer time for this study was provided by the Center for High Performance Computing (CHPC) at the University of Utah.

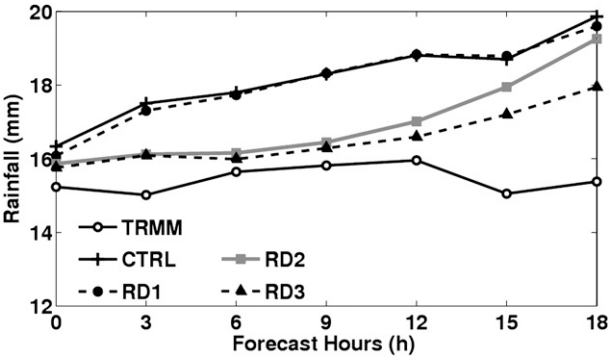

FIG. 13. Time series of the 3-h accumulated rainfall (mm) averaged over an area within 250-km distance from the storm center from different simulations and the TRMM 3B42 products between 0600 UTC 8 Jul and 0000 UTC 9 Jul 2005.

This study is supported by the NASA TCSP and NAMMA programs, NASA EOS program Grant NNX08AD32G, and ONR Grant N00014-08-1-0308.

REFERENCES

Aberson, S. D., and B. J. Etherton, 2006: Targeting and data assimilation studies during Hurricane Humberto (2001). *J. Atmos. Sci.,* **63,** 175–186.

Barker, D. M., W. Huang, Y. R. Guo, and Q. N. Xiao, 2004a: A three-dimensional (3DVAR) data assimilation system for use with MM5: Implementation and initial results. *Mon. Wea. Rev.,* **132,** 897–914.

——, M.-S. Lee, Y.-R. Guo, W. Huang, Q.-N. Xiao, and R. Rizvi, 2004b: WRF variational data assimilation development at NCAR. Preprints, *WRF/MM5 Users' Workshop,* Boulder, CO, 5.1.

Beven, J., cited 2005: Tropical cyclone report: Hurricane Dennis, 4–13 July 2005. National Hurricane Center Report, 25 pp. [Available online at http://www.nhc.noaa.gov/pdf/TCR-AL042005_Dennis.pdf.]

Courtier, P., J. N. Thepaut, and A. Hollingsworth, 1994: A strategy for operational implementation of 4D-Var using an incremental approach. *Quart. J. Roy. Meteor. Soc.,* **120,** 1367–1387.

Dudhia, J., 1989: Numerical study of convection observed during the Winter Monsoon Experiment using a mesoscale two-dimensional model. *J. Atmos. Sci.,* **46,** 3077–3107.

Franklin, J. L., S. J. Lord, and F. D. Marks Jr., 1988: Dropwindsonde and radar observations of the eye of Hurricane Gloria (1985). *Mon. Wea. Rev.,* **116,** 1237–1244.

Gamache, J. F., 2005: Real-time dissemination of hurricane wind fields determined from airborne Doppler radar. National Hurricane Center Tropical Prediction Center JHT Project Final Rep, 38 pp. [Available online at http://www.nhc.noaa.gov/jht/2003-2005reports/DOPLRgamache_JHTfinalreport.pdf.]

Gao, J., M. Xue, A. Shapiro, and K. K. Droegemeier, 1999: A variational method for the analysis of three-dimensional wind fields from two Doppler radars. *Mon. Wea. Rev.,* **127,** 2128–2142.

Grell, G. A., and D. Dévényi, 2002: A generalized approach to parameterizing convection combining ensemble and data assimilation techniques. *Geophys. Res. Lett.,* **29,** 1693, doi:10.1029/2002GL015311.

Halverson, J., and Coauthors, 2007: NASA's Tropical Cloud Systems and Processes experiment. *Bull. Amer. Meteor. Soc.,* **88,** 867–882.

Hendricks, E. A., M. T. Montgomery, and C. A. Davis, 2004: The role of "vortical" hot towers in the formation of Tropical Cyclone Diana (1984). *J. Atmos. Sci.,* **61,** 1209–1232.

Hong, S.-Y., and J.-O. Lim, 2006: The WRF single-moment 6-class microphysics scheme (WSM6). *J. Korean Meteor. Soc.,* **42,** 129–151.

Houze, R. A., Jr., and Coauthors, 2006: The Hurricane Rainband and Intensity Change Experiment: Observations and modeling of Hurricanes Katrina, Ophelia, and Rita. *Bull. Amer. Meteor. Soc.,* **87,** 1503–1521.

——, S. S. Chen, B. F. Smull, W.-C. Lee, and M. M. Bell, 2007: Hurricane intensity and eyewall replacement. *Science,* **315,** 1235–1239.

Huffman, G. J., and Coauthors, 2007: The TRMM Multisatellite Precipitation Analysis (TMPA): Quasi-global, multiyear, combined-sensor precipitation estimates at fine scales. *J. Hydrometeor.,* **8,** 38–55.

Janjic, Z. I., 2002: Nonsingular implementation of the Mellor-Yamada level 2.5 scheme in the NCEP global model. NCEP Office Note 437, 61 pp.

Jordan, C. L., 1961: Marked changes in the characteristics of the eye of intense typhoons between the deepening and filling stages. *J. Meteor.,* **18,** 779–789.

Kakar, R., M. Goodman, R. Hood, and A. Guillory, 2006: Overview of the Convection and Moisture Experiment (CAMEX). *J. Atmos. Sci.,* **63,** 5–18.

Kessler, E., 1969: *On the Distribution and Continuity of Water Substance in Atmospheric Circulation. Meteor. Monogr.,* No. 32, Amer. Meteor. Soc., 84 pp.

Kossin, J. P., and M. D. Eastin, 2001: Two distinct regimes in the kinematic and thermodynamic structure of the hurricane eye and eyewall. *J. Atmos. Sci.,* **58,** 1079–1090.

Landsea, C. W., 1993: A climatology of intense (or major) Atlantic hurricanes. *Mon. Wea. Rev.,* **121,** 1703–1713.

Lord, S. J., H. E. Willoughby, and J. M. Piotrowicz, 1984: Role of a parameterized ice-phase microphysics in an axisymmetric, nonhydrostatic tropical cyclone model. *J. Atmos. Sci.,* **41,** 2836–2848.

Lorenc, A. C., 1986: Analysis methods for numerical weather prediction. *Quart. J. Roy. Meteor. Soc.,* **112,** 1177–1194.

Marks, F. D., 2003: State of the science: Radar view of tropical cyclones. *Radar and Atmospheric Science: A Collection of Essays in Honor of David Atlas, Meteor. Monogr.,* No. 52, Amer. Meteor. Soc., 33–74.

——, P. G. Black, M. T. Montgomery, and R. W. Burpee, 2007: Structure of the eye and eyewall of Hurricane Hugo (1989). *Mon. Wea. Rev.,* **136,** 1237–1259.

McFarquhar, G. M., and R. A. Black, 2004: Observations of particle size and phase in tropical cyclones: Implications for mesoscale modeling of microphysical processes. *J. Atmos. Sci.,* **61,** 422–439.

——, H. Zhang, G. Heymsfield, R. Hood, J. Dudhia, J. B. Halverson, and F. Marks, 2006: Factors affecting the evolution of Hurricane Erin (2001) and the distributions of hydrometeors: Role of microphysical processes. *J. Atmos. Sci.,* **63,** 127–150.

Mlawer, E. J., S. J. Taubman, P. D. Brown, M. J. Iacono, and S. A. Clough, 1997: Radiative transfer for inhomogeneous atmosphere: RRTM, a validated correlated-k model for the long-wave. *J. Geophys. Res.,* **102** (D14), 16 663–16 682.

Montgomery, M. T., M. E. Nicholls, T. A. Cram, and A. Saunders, 2006: A vortical hot tower route to tropical cyclogenesis. *J. Atmos. Sci.,* **63,** 355–386.

Parrish, D. F., and J. C. Derber, 1992: The National Meteorological Center's spectral statistical-interpolation analysis system. *Mon. Wea. Rev.,* **120,** 1747–1763.

Persing, J., and M. T. Montgomery, 2003: Hurricane superintensity. *J. Atmos. Sci.,* **60,** 2349–2371.

Pu, Z., X. Li, C. Velden, S. Aberson, and W. T. Liu, 2008: Impact of aircraft dropsonde and satellite wind data on the numerical simulation of two landfalling tropical storms during the Tropical Cloud Systems and Processes Experiment. *Wea. Forecasting,* **23,** 62–79.

——, ——, and E. J. Zipser, 2009: Diagnosis of the initial and forecast errors in the numerical simulation of the rapid intensification of Hurricane Emily (2005). *Wea. Forecasting,* **24,** 1255–1270.

Rogers, R., and Coauthors, 2006: The Intensity Forecasting Experiment: A NOAA multiyear field program for improving tropical cyclone intensity forecasts. *Bull. Amer. Meteor. Soc.,* **87,** 1523–1537.

——, M. L. Black, S. S. Chen, and R. A. Black, 2007: An evaluation of microphysics fields from mesoscale model simulations of tropical cyclones. Part I: Comparisons with observations. *J. Atmos. Sci.,* **64,** 1811–1834.

Skamarock, W. C., J. B. Klemp, J. Dudhia, D. O. Gill, D. M. Barker, W. Wang, and J. G. Powers, 2005: A description of the advanced research WRF version 2. NCAR Tech. Note NCAR/TN-468+STR, 88 pp.

Sun, J., 2005: Initialization and numerical forecasting of a supercell storm observed during STEPS. *Mon. Wea. Rev.,* **133,** 793–813.

——, and N. A. Crook, 1997: Dynamical and microphysical retrieval from Doppler radar observations using a cloud model and its adjoint. Part I: Model development and simulated data experiments. *J. Atmos. Sci.,* **54,** 1642–1661.

——, and ——, 1998: Dynamical and microphysical retrieval from Doppler radar observations using a cloud model and its adjoint. Part II: Retrieval experiments of an observed Florida convective storm. *J. Atmos. Sci.,* **55,** 835–852.

Wang, Y., 2002: Vortex Rossby waves in a numerically simulated tropical cyclone. Part II: The role in tropical cyclone structure and intensity changes. *J. Atmos. Sci.,* **59,** 1239–1262.

Weygandt, S. S., A. Shapiro, and K. K. Droegemeier, 2002: Retrieval of model initial fields from single-Doppler observations of a supercell thunderstorm. Part II: Thermodynamic retrieval and numerical prediction. *Mon. Wea. Rev.,* **130,** 454–476.

Wu, W.-S., R. J. Purser, and D. F. Parrish, 2002: Three-dimensional variational analysis with spatially inhomogeneous covariances. *Mon. Wea. Rev.,* **130,** 2905–2916.

Xiao, Q., Y.-H. Kuo, J. Sun, W.-C. Lee, E. Lim, Y.-R. Guo, and D. M. Barker, 2005: Assimilation of Doppler radar observations with a regional 3DVAR system: Impact of Doppler velocities on forecasts of a heavy rainfall case. *J. Appl. Meteor.,* **44,** 768–788.

——, ——, ——, ——, D. M. Barker, and E. Lim, 2007: An approach of radar reflectivity data assimilation and its assessment with the inland QPF of Typhoon Rusa (2002) at landfall. *J. Appl. Meteor. Climatol.,* **46,** 14–22.

——, X. Zhang, C. A. Davis, J. Tuttle, G. J. Holland, and P. J. Fitzpatrick, 2009: Experiments of hurricane initialization with airborne Doppler radar data for the advanced research hurricane WRF (AHW) model. *Mon. Wea. Rev.,* **137,** 2758–2777.

Zhao, Q., and Y. Jin, 2008: High-resolution radar data assimilation for Hurricane Isabel (2003) at landfall. *Bull. Amer. Meteor. Soc.,* **89,** 1355–1372.